www.ietdl.org

Published in IET Image Processing
Received on 6th May 2012
Revised on 15th December 2012
Accepted on 14th January 2013
doi: 10.1049/iet-ipr.2012.0203

ISSN 1751-9659

Colour and texture feature-based image retrieval by using Hadamard matrix in discrete wavelet transform

Hassan Farsi, Sajad Mohamadzadeh

Department of Electronics and Communications Engineering, University of Birjand, Birjand, Iran
E-mail: hfarsi@birjand.ac.ir

Abstract: Image retrieval is one of the most applicable image processing techniques, which has been used extensively. Feature extraction is one of the most important procedures used for interpretation and indexing images in content-based image retrieval systems. Effective storage, indexing and managing a large number of image collections is a critical challenge in computer systems. There are many proposed methods to overcome these problems. However, the rate of accurate image retrieval and speed of retrieval is still an interesting field of research. In this study, the authors propose a new method based on combination of Hadamard matrix and discrete wavelet transform (HDWT) in hue-min-max-difference colour space. An average normalised rank and combination of precision and recall are considered as metrics to evaluate and compare the proposed method against different methods. The obtained results show that the use of HDWT provides better performance in comparison with Haar discrete wavelet transform, colour layout descriptor, dominant colour descriptor and scalable colour descriptor, Padua point and histogram intersection.

1 Introduction

Today, growth of technology, low cost storage and use of the internet causes the number of digital images such as medical, signature, nature, satellite images and so on to incredibly increase. Therefore storage, search and organisation of digital images are highly in demand. Designing a search image mechanism based on user requirements to find images related to user demand has become an important research topic in this field. Image retrieval is a process that searches for a query image among image datasets. Owing to various applications of image retrieval, many researchers in different subjects such as image processing, multimedia system, digital library, astronomy, medical sciences and architecture are working in this area. An image retrieval system is able to find an appropriate image according to query image and human perception. Dataset management (based on text feature) and machine vision (based on vision feature) are the two main research fields, which study the image retrieval system [1, 2].

In the beginning of 1990, because of rise in the number of capacious images used in the internet and also because of the shortcomings mentioned above, text-based image retrieval was an inefficient method and demand for content-based image retrieval (CBIR) appeared [3, 4]. CBIR techniques are one of the most applicable and increasingly important topics in multimedia information systems [5]. The image retrieval systems consist of three main parts: the first and the most important part is feature extraction. Feature extraction is one of the most important procedures used for interpretation and indexing images in CBIR systems [6]. This part produces the feature vector for all images in the dataset, which represents image concept for image classification. The size of the feature vector has to be smaller than the image size. This results in minimisation of search time, simple search process and retrieval of same image as quickly as possible. The second part is called indexing. This part classifies the images using the extracted features. Image Indexing is known as characterisation of images based on some features of images [7]. Retrieval part is the last part of the image retrieval system. This part extracts the feature vectors of query image, calculates the distance between the feature vector of query image and the obtained feature vectors of all images in the dataset using similarity measure and finds similar images [8].

There are many proposed methods and approaches for classification, indexing, search and retrieval of visual information based on analysis of low-level image features such as colour, texture, shape etc. [8]. The combination of these features showed more efficient performance in image retrieval systems [3].

Colour is one of the most common and determinant features used in the image retrieval system, which is stable against direction variations, size of image and background complexity [9]. Colour space is needed to have the following characteristics: (i) independent from hardware, (ii) having uniform perception, which means the distance between colours has to be proportional with human perception distinctions, (iii) understandable and imaginable for user [10]. In this article, we have used hue-min-max-difference (HMMD) and red, green and blue (RGB) colour spaces, because these colour spaces are robust against image distortion in comparison with other colour spaces [10].

Although the methods of colour feature extraction require low complexity for retrieval, they do not consider distribution of colour location [5]. Therefore image retrieval based on texture is generally considered. Owing to the importance of texture feature, it has been widely used in different fields such as pattern recognition, machine vision and image retrieval [5]. Different methods have been proposed for description of image texture. Jain and Tuceryan have divided the texture analysis methods into four groups [11]: statistical [12], geometrical or structural [13–15], model-based and signal processing methods. In this paper, we have used the signal processing method because it results in higher performance in comparison with the other methods mentioned above [16, 17]. We use wavelet transform because it is an appropriate choice for replacement of Fourier transform. It provides orthonormal bases in two-dimensional spaces and in spite of Fourier transform it can be localised in time and frequency domains and extracts accurately local information of signal. Therefore using the wavelet transform in same applications, where the signal has non-stationary characteristics with high-frequency components, is more appropriate than Fourier transform. Wavelet transform theory has grown up during the last year and it is now used in different fields and applications. Discrete wavelet transform (DWT) applied on discrete signals causes the speed of the transform to increase [16, 17].

In spite of proposing various methods in image retrieval during recent years, there is no efficient and perfect algorithm to represent human perception for interpretation of images. The original image is created by an array of pixel values, which has little coordination with visual reactions. The aim of this paper is to propose a new algorithm for searching in different image datasets (independent from image dataset) with high accurate retrieval and low complexity or high-speed retrieval. We have proposed a new CBIR system and it is evaluated by three varied datasets with different sizes. Each dataset has individual characteristics and contains different images independent of other datasets.

The proposed method combines new colour and texture features to increase retrieval performance. We define the average of red, green and blue planes as intensity plane, red, green and blue planes as RGB planes and minimum, maximum and difference planes as HMMD planes. Then, we extract some texture features from intensity, RGB and HMMD planes, separately. The HMMD colour space is described in Section 2.1. The size of feature vectors and speed of retrieval are important aspects in performance of image retrieval. The proposed method uses Hadamard matrix [18] and DWT [19] (HDWT). Applying the proposed method on the datasets results in reduction of feature vector size and storage space in high-level wavelet transform.

This paper has been organised as follows. In Section 2, the proposed CBIR system, HMMD colour space and feature extraction method by using DWT and Hadamard matrix and similarity measurement have been explained. Image retrieval using the proposed system has been described and the obtained results in the three datasets have been presented in Section 3. Finally, the conclusion is drawn in Section 4.

2 Proposed CBIR system

Texture, colour and shape features are basic features used in CBIR systems. Texture and colour features are easy for computing similarity. Some CBIR systems have combined texture and colour features to provide better performance and automatically retrieved relevant images from a large image dataset [20]. Therefore we have used a combination of colour and texture features. The standard CBIR systems involve two important parts [20]. The first part extracts image features, which generates a feature vector of each image from the dataset and represents the content of image accurately. The size of feature vectors must be extremely smaller than the primary image. Similarity measurement is the second part of CBIR systems. This part computes the distance between the query image and each image of the dataset by using feature vectors of query image and each image of the dataset to obtain similar images. Therefore small vector size increases the speed of retrieval and reduces storage memory. The proposed CBIR system is conceptually described by the framework depicted in Fig. 1.

In this method, before the extraction of HDWT feature and the generation of feature vector, all images are resized to $256 \times 256 \times 3$, and intensity, RGB and HMMD planes are generated with size of 256×256. Therefore by applying HDWT to each image, dataset feature vectors and query feature vectors are constructed. Then, the distance between query feature vector and feature vector of each image in the dataset is computed and similar images are drawn.

2.1 HMMD colour space

The HMMD is a new colour space supported by MPEG-7 [10]. The hue (H) represents the dominant spectral component colour in its pure form (as green, red or yellow). The hue is measured by the angle around the vertical axis, with red corresponding to 0°. The colour space is depicted using the double cone structure as shown in Fig. 2. Min (M) and max (M) are the minimum and maximum value between the red, green and blue values, respectively. The difference (D) component is presented as the difference between max and min values. HMMD space colour can be

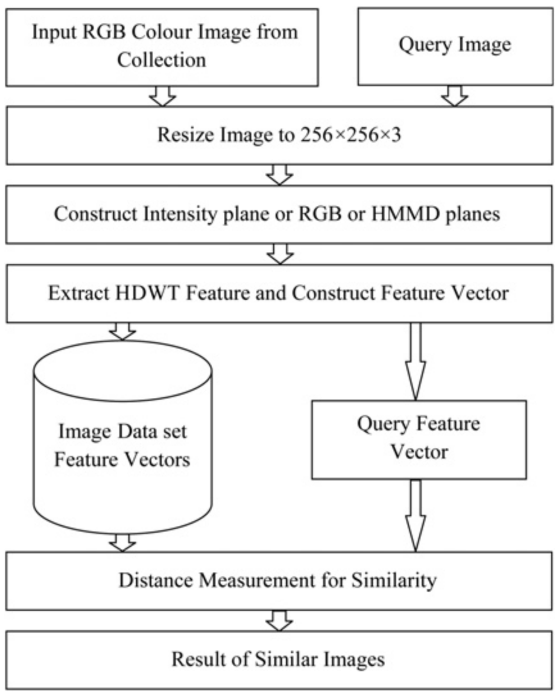

Fig. 1 *Block diagram of the proposed CBIR system*

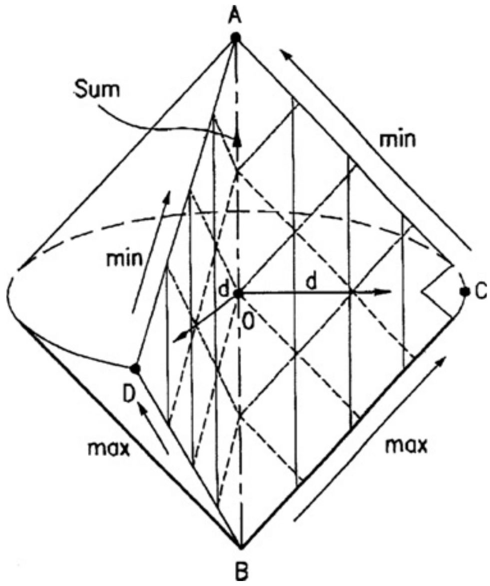

Fig. 2 *HMMD colour space [10]*

described completely by using three of the four components. Therefore we have used min, max and difference components, because *H* component has been shown not to have a beneficial effect in combination with Euclidean distance because of its cyclic nature [10]. In the MPEG-7 core experiments for image retrieval, it has been shown that the HMMD colour space is more effective and more favourable than HSV colour space [10]. Note that the HMMD colour space is a slight twist on HSI colour space, where the difference component is scaled by the intensity value [10].

2.2 Feature extraction method

We have combined HDWT to extract the texture features of each image. The flowchart of the HDWT method has been represented in Fig. 3 and the steps are represented as follows:

Step 1: After reading intensity or RGB or HMMD planes, we apply DWT on each RGB, HMMD and intensity plane, separately with size of $N \times N$ to generate approximation (low–low), horizontal (low–high), vertical (high–low) and diagonal (high–high) components. We use approximation components for the next step because wavelet transform analyses the signal at various frequency bands and gives higher frequency resolution and lower time resolution at lower frequencies [17]. For a given image with size of $N \times N$, the two-dimensional wavelet transform includes $\log_2{}^N$ stages. The first stage provides four sets of coefficients known as approximation coefficients cA1, horizontal coefficients cH1, vertical coefficients cV1 and diagonal coefficients cD1. These sets are computed by convolving columns or rows of images with the low-pass filter for approximation, and with the high-pass filter, which are followed by dyadic decimation (down-sampling). The length of these filters is $2n$ samples. Therefore if the length of an image is N, then the length of output signal of low-pass and high-pass filters will be $N + 2n - 1$ [19]. Fig. 4 describes the flowchart of the basic decomposition of wavelet transform for an input image.
Step 2: Construction of modified approximation components by multiplying approximation components and Hadamard matrix with size of approximation component. Hadamard matrices are square matrices whose entries are either +1 or −1 and their rows are mutually orthogonal [18]. Geometrically, this means that every two different rows in a Hadamard matrix represent two perpendicular vectors, whereas in combinatorial terms, it shows that every two different rows have matching entries in exactly half of their columns and mismatched entries in the remaining columns. Equivalently, a Hadamard matrix has maximal determinant among matrices with entries of absolute value less than or equal to 1 and therefore it can be considered as an external solution of Hadamard's maximal determinant problem. Also, Hadamard matrices can be reduced to subtraction and addition operations (no division or multiplication is needed) [18]. This allows the use of simpler hardware to calculate the transform and increases the speed of retrieval because of low complexity. Fig. 5 represents designing Hadamard matrices.

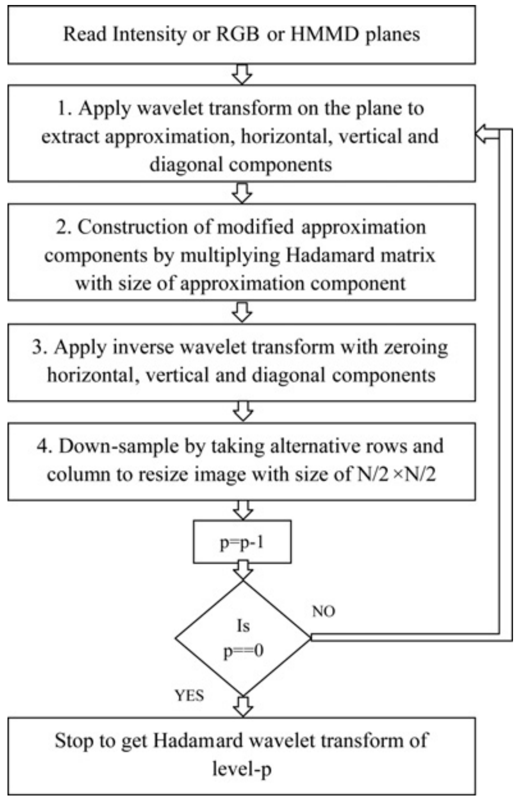

Fig. 3 *Generating HDWT feature level p*

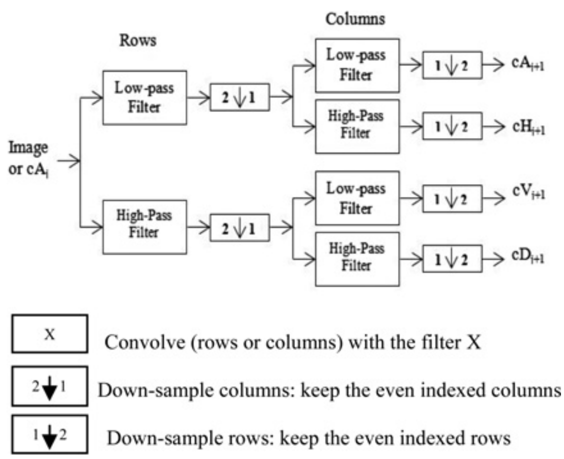

Fig. 4 *Decomposition of the image by wavelet transform*

$$H_2 = \begin{bmatrix} 1 & 1 \\ -1 & 1 \end{bmatrix}$$

$$H_4 = \begin{bmatrix} H_2 & H_2 \\ -H_2 & H_2 \end{bmatrix}$$

$$= \begin{bmatrix} \begin{bmatrix} 1 & 1 \\ -1 & 1 \end{bmatrix} & \begin{bmatrix} 1 & 1 \\ -1 & 1 \end{bmatrix} \\ -\begin{bmatrix} 1 & 1 \\ -1 & 1 \end{bmatrix} & \begin{bmatrix} 1 & 1 \\ -1 & 1 \end{bmatrix} \end{bmatrix}$$

$$= \begin{bmatrix} 1 & 1 & 1 & 1 \\ -1 & 1 & -1 & 1 \\ -1 & -1 & 1 & 1 \\ 1 & -1 & -1 & 1 \end{bmatrix}$$

Fig. 5 *Hadamard matrices [18]*

Step 3: Construction of modified plane from step 2 by applying inverse wavelet transform with modified approximation components, zeroing horizontal, vertical and diagonal components. A new image is constructed by using inverse wavelet whereas some information disappears because of removing horizontal, vertical and diagonal components. We need a new image in the next level to construct new approximation components.
Step 4: To take alternative rows and columns by down-sampling the output of step 3 with size of $N/2 \times N/2$. Down-sampling reduces the size of feature vector, which is very important for increasing the speed of retrieval.
Step 5: To construct HDWT feature of level p by repeating steps 2–4, 'p' times on each plane.
Step 6: Using approximation components of level p resulting in step 2 as HDWT feature of level p.

We generate feature vectors of dataset image by applying HDWT level 1, level 2, …, level 7 and store approximation component as feature vectors for each image. Size of feature vector is $(N/(2\hat{}p)) \times (N/(2\hat{}p))$ in HDWT level p.

2.3 Similarity measure

Euclidean distance is a simple and fast metric, therefore it is the most common metric used to compute match or similarity value in CBIR systems to obtain relevant images. If FVD and FVQ are two-dimensional feature vectors of dataset image and query image, respectively, then the Euclidean distance of these feature vectors is obtained by

$$\text{ED} = \sqrt{\sum_{i=1}^{n} \left(\text{FVD}_i - \text{FVQ}_i\right)^2} \qquad (1)$$

3 Experimental results

3.1 Datasets and evaluation measures

In order to evaluate the proposed method in image retrieval, we consider three different datasets: (i) Corel dataset [21] including 1000 variable size images classified into 11 classes of human beings, horse, elephant, flower, bus, man-made things and natural scenery. (ii) The Amsterdam Library of Object Images [22] (ALOIs) dataset including 72 000 variable size images in 1000 classes. (iii) MPEG-7 dataset [23] including 1400 variable size images in 70 classes. The MPEG-7 is a difficult dataset for colour-based image retrieval. Instead of objects, its images are composed of photos and sequences of video frames. Also, we used only the photos part of each image. All classes in each dataset are well balanced. We have tried to collect diverse datasets to evaluate the proposed method.

After collection of the image datasets, we select five, three and four random images from each class in Corel, ALOI and MPEG-7 datasets, respectively, as query images to evaluate the proposed method. Intensity, RGB and HMMD planes are used to generate intensity-HDWT, RGB-HDWT and HMMD-HDWT feature vectors, respectively, to get respective images at different levels. Also, we have used the proposed method to extract query feature and to generate feature vector of query image. The relevant images are then retrieved by comparing the feature vector of query with the feature vector dataset in level p by using Euclidean distance as the similarity measure. The Euclidean distances are sorted to find the best relevant images in the dataset. We have compared performance of the proposed method with three evaluation metrics as follows:

1. The normalised rank is a performance measure used to summarise system performance into a scalar value. The normalised rank for a given image ranking Ω_α^i, denoted as $\text{Rank}(H_\alpha)$, is defined as

$$\text{Rank}(H_\alpha) = \frac{1}{NN_\alpha}\left(\sum_{i=1}^{N_\alpha} \Omega_\alpha^i - \frac{N_\alpha(N_\alpha - 1)}{2}\right) \qquad (2)$$

where N is the number of images in the dataset, N_α is the number of relevant images for the query H_α, and Ω_α^i is the rank in which the ith image is retrieved. This measure is 0 for perfect performance and approaches to 1 as performance worsens, where 0.5 is equivalent to a random retrieval [24]. The average normalised rank (ANR) for the full dataset is given by

$$\text{ANR} = \frac{1}{N}\sum_{\alpha=1}^{N} \text{Rank}(H_\alpha) \qquad (3)$$

2. Precision and recall are used for evaluation of most CBIR systems. Precision is the fraction of returned images that are relevant to the query image. Recall is the fraction of returned relevant images with respect to the total number of relevant images in the dataset according to a priori knowledge. If we denote T as the set of returned images and R as the set of all images relevant to the query image, then the precision and recall criteria are given by using (4) and (5), respectively [24].

$$\text{Precision} = \frac{|T \cap R|}{|T|} \qquad (4)$$

$$\text{Recall} = \frac{|T \cap R|}{|R|} \qquad (5)$$

The numbers of relevant images are computed and the precision and recall in each number of retrieved images for all query images are obtained. We next consider the average of these precisions and recalls for each number of retrieved images as the precision and recall of each method for each number of retrieved images.

3. We use various methods to evaluate the proposed system. Montagna and Finlayson [9] have proposed a method using the combination of precision and recall criteria as the performance measures for CBIR systems. According to Montagna and Finlayson [9], the following measures have been adopted:

- *P* (1/3), precision at 33.33% recall (i.e. precision after retrieving 1/3 of the relevant documents).
- *P* (2/3), precision at 66.66% recall (i.e. precision after retrieving 2/3 of the relevant documents).
- *P* (1), precision at 100% recall (i.e. precision after retrieving all of the relevant documents, *P*(1) is the percent of crossover point of precision and recall).

We use these values because precision and recall are considered in relation to each other and they are not meaningful if taken separately.

3.2 Indexing results

As an example, the average precision and recall for intensity-HDWT, RGB-HDWT and HMMD-HDWT, in Corel dataset are obtained and plotted by grouping the number of retrieved images in Figs. 6–8, respectively. According to these figures, it is obvious that precision is decreased and recall is increased by increasing the number of retrieved images. Also, by increasing wavelet level until level 5, precision and recall are increased but they are decreased after level 5. For example, the precisions of HMMD-HDWT level 1, 3 and 5 are 0.451, 0.466 and 0.492 in 88 retrieved images, respectively, but the precision of HMM-HDWT level 7 is 0.409. Therefore precision and recall level 5 of wavelet methods are better than other wavelet levels and we have compared wavelet methods in level 5. Moreover, it is observed that the precision of intensity, RGB and HMMD HDWT level 5 are 0.448 and 0.472, respectively, whereas the precision of HMMD-HDWT level 5 is 0.492 in 88 retrieved images. Therefore the proposed HMMD-HDWT method provides better performance rather than intensity-HDWT and RGB-HDWT. In all levels except for level 7, HMMD-HDWT has better performance than RGB-HDWT and intensity-HDWT.

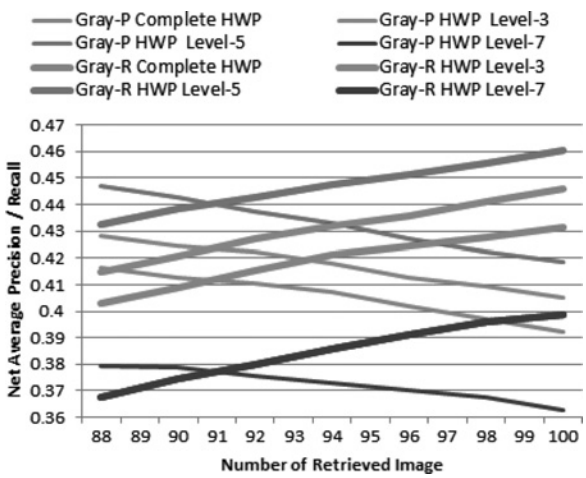

Fig. 6 *Intensity HDWT method precision\recall in Corel dataset*

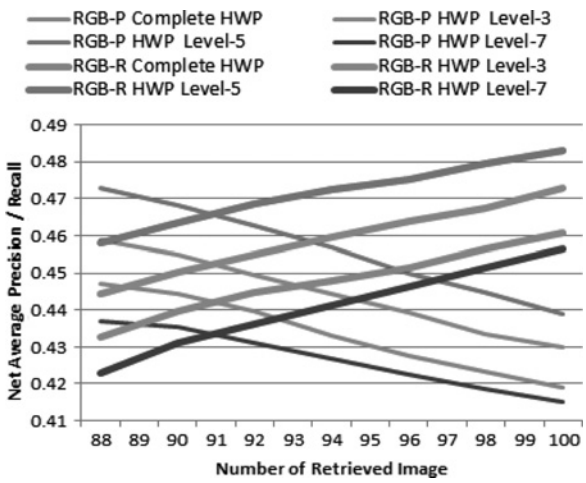

Fig. 7 *RGB-HDWT method precision\recall in Corel dataset*

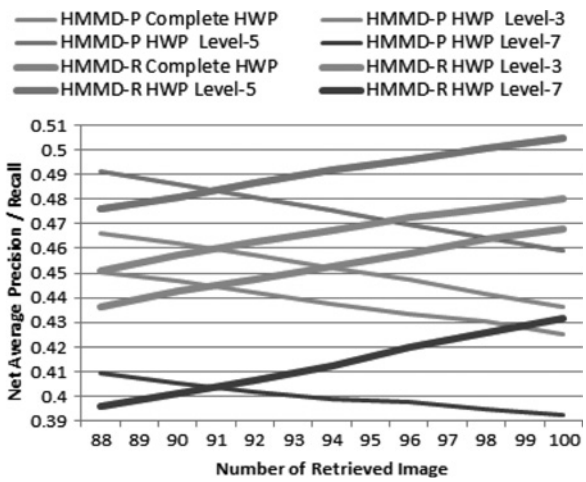

Fig. 8 *HMMD-HDWT method precision\recall in Corel dataset*

The size of feature vector, ANR, *P*(1/3), *P*(2/3) and *P*(1) for different levels of intensity and RGB Haar wavelet [25], intensity, RGB and HMMD HDWT, colour layout descriptor (CLD) [10, 26], dominant colour descriptor (DCD) [27], scalable colour descriptor (SCD) [10], Padua point (PP) [9] and histogram intersection (HI) [9] methods have been represented in Tables 1–3, for Corel, ALOI and MPEG-7 datasets, respectively. As observed, the size of the feature vector is decreased by increasing wavelet level but '*p*' only increases until level 5. However, the size of the feature vector is 4 in level 7, but the *P*(1) (40.33% of *P*(1) of HMMD-HDWT in Corel dataset) is less than level 1 with 16 384 size of feature vector where *P*(1) of HMMD-HDWT level 1 in Corel dataset is 44.54%. In Tables 1–3, it is also observed that ANR are decreased until level 5. It is obvious that level 5 of each five wavelet methods with size of feature vector equal to 64 has higher performance than other levels in each wavelet method in the three datasets.

In Tables 1–3, the best scores for each metric are in bold face. Table 1 summarises the test results on the Corel dataset. In this experiment, HMMD-HDWT has best *P*(1/3), *P*(2/3) and *P*(1) for all methods. The CLD method has better ANR than HMMD-HDWT, but CLD ANR is only 0.002 lower than RGB-HDWT level 5. In Table 2, we show the results of the same experiment run on the ALOI dataset.

doi: 10.1049/iet-ipr.2012.0203

Table 1 Size of feature vector, ANR, P(1/3), P(2/3) and P(1) of different methods in Corel dataset

Type	Level	Size of feature vector	ANR	P(1/3), %	P(2/3), %	P(1), %
intensity-Haar	1	16 384	0.261	48.54	40.33	37.28
	3	1024	0.256	50.33	44.12	38.10
	5	64	0.255	51.44	46.54	38.54
	7	4	0.265	45.76	36.89	34.55
RGB-Haar	1	3 × 16 384	0.232	53.21	47.44	41.27
	3	3 × 1024	0.226	55.98	49.33	42.09
	5	3 × 64	0.221	58.33	50.66	42.57
	7	3 × 4	0.224	49.23	41.97	39.23
intensity-HDWT	1	16 384	0.260	51.81	45.33	41.18
	3	1024	0.256	53.82	47.09	42.42
	5	64	0.253	55.46	48.88	43.42
	7	4	0.264	46.18	41.63	37.94
RGB-HDWT	1	3 × 16 384	0.232	58.73	51.12	44.23
	3	3 × 1024	0.226	61.03	52.55	45.33
	5	3 × 64	0.221	62.36	54.33	46.58
	7	3 × 4	0.228	55.03	48.03	43.41
HMMD-HDWT	1	3 × 16 384	0.243	57.21	50.24	44.54
	3	3 × 1024	0.238	59.21	52.27	45.98
	5	3 × 64	0.234	62.73	55.52	48.34
	7	3 × 4	0.253	53.82	45.67	40.33
CLD	–	12	0.219	62.46	55.06	41.82
DCD	–	32	0.243	55.03	44.58	36.37
SCD	–	121	0.316	51.58	41.85	33.65
PP30	–	496	0.306	41.54	36.56	28.65
HI	–	1024	0.291	46.63	36.67	29.92

Table 2 Size of feature vector, ANR, P(1/3), P(2/3) and P(1) of different methods in ALOI dataset

Type	Level	Size of feature vector	ANR	P(1/3), %	P(2/3), %	P(1), %
intensity-Haar	1	16 384	0.104	72.45	56.34	48.75
	3	1024	0.091	74.23	63.35	50.06
	5	64	0.079	77.66	66.09	52.84
	7	4	0.106	59.88	40.16	38.91
RGB-Haar	1	3 × 16 384	0.084	76.78	61.69	51.77
	3	3 × 1024	0.082	79.64	64.72	56.52
	5	3 × 64	0.072	81.53	68.41	57.65
	7	3 × 4	0.085	65.24	49.42	40.89
intensity-HDWT	1	16384	0.101	81.38	67.08	57.60
	3	1024	0.088	85.04	71.32	61.26
	5	64	0.076	87.06	73.18	62.68
	7	4	0.105	61.78	49.26	41.04
RGB-HDWT	1	3 × 16 384	0.080	85.75	72.87	60.63
	3	3 × 1024	0.079	90.16	75.98	64.32
	5	3 × 64	0.071	90.36	76.73	65.53
	7	3 × 4	0.081	74.52	57.61	48.16
HMMD-HDWT	1	3 × 16 384	0.084	99.95	79.88	77.54
	3	3 × 1024	0.077	100	92.59	80.32
	5	3 × 64	0.062	100	94.66	83.14
	7	3 × 4	0.081	87.03	64.73	62.80
CLD	–	12	0.664	20.68	19.03	17.56
DCD	–	32	0.344	55.71	48.98	41.87
SCD	–	121	0.232	61.68	52.70	43.55
PP30	–	496	0.764	50.32	33.21	7.71
HI	–	1024	0.772	47.57	29.43	6.77

Table 3 Size of feature vector, ANR, P(1/3), P(2/3) and P(1) of different methods in MPEG-7 dataset

Type	Level	Size of feature vector	ANR	P(1/3), %	P(2/3), %	P(1), %
Haar	1	16 384	0.171	67.07	57.64	45.34
	3	1024	0.165	68.12	58.02	47.31
	5	64	0.159	69.56	60.01	48.14
	7	4	0.179	49.80	40.53	32.99
HDWT	1	16 384	0.171	73.82	62.14	51.51
	3	1024	0.165	74.48	62.24	52.35
	5	64	0.159	74.69	63.13	54.68
	7	4	0.179	55.86	45.38	38.07
PP30	–	496	0.179	80.22	60.21	37.21
HI	–	1024	0.159	90.32	81.22	57.56

Once again, it is observed that HMMD-HDWT has best ANR and $P(1/3)$, $P(2/3)$ and $P(1)$. In Table 3, we show the results of Haar, HDWT, PP and HI experiment run on the MPEG-7 dataset. However in this table, ANR of HI, Haar and HDWT are identical but HI method has better $P(1/3)$, $P(2/3)$ and $P(1)$ than other methods. However, $P(1/3)$, $P(2/3)$ and $P(1)$ HI method is better than HDWT level 5 [>3% in $P(1)$], but the size of feature vector HI is more than HDWT (>16 times). Therefore the proposed HMMD-HDWT method in level 5 has even better performance than intensity and RGB Haar, intensity and RGB HDWT, CLD, DCD, SCD, PP and HI. Therefore HMMD-HDWT technique can be considered as a powerful method rather than wavelet methods and other methods.

4 Conclusion

Image retrieval is an applicable technique used to find relevant images in a large image dataset. By increasing the size of the dataset the challenge of average reduction in precision and recall and speed of retrieval become more serious. In this paper, we proposed a new method based on HDWT in HMMD and RGB colour spaces to improve the performance of image retrieval. We used an average of three planes of red, green and blue to generate an intensity plane and considering red, green and blue planes separately to generate RGB planes and considering minimum, maximum and difference planes separately to generate HMMD planes to test the proposed method. The obtained results showed using HMMD colour space and Hadamard transform in DWT that there could be improvement in the performance of image retrieval in the three datasets. Specially, HMMD-HDWT in level 5 provided better performance in comparison with other methods. Moreover, the HDWT method reduced the size of feature vectors and storage space and therefore reduced the computation time extremely in high level of HDWT and provided better performance. The reason for reduction of computation time and complexity is that by using a high level of HDWT, for example, level 5 of HDWT, the size of feature vector is 64 (8×8) whereas the original size of image is 65 536 (256×256).

5 References

1 Feng, J., Mingjing, L., Hong-Jiang, Z., Bo, Z.: 'A unified framework for image retrieval using keyword and visual features', *IEEE Trans. Image Process.*, 2005, **14**, (7), pp. 979–989

2 Liu, Y., Zhang, D., Lu, G., Ma, W.Y.: 'A survey of content-based image retrieval with high-level semantics', *Pattern Recognit.*, 2007, **40**, (1), pp. 262–282

3 Li, F., Dai, Q., Xu W., Er G.: 'Multi-label neighborhood propagation for region-based image retrieval', *IEEE Trans. Multimed.*, 2008, **10**, (8), pp. 1592–1604

4 Chen, S.X., Li, F.W., Zhu, W.L.: 'Fast searching algorithm for vector quantization based on features of vector and sub-vector', *IET Image Process.*, 2008, **2**, (6), pp. 275–285

5 Lin, C.-H., Liu, C.-W., Chen, H.-Y.: 'Image retrieval and classification using adaptive local binary patterns based on texture features', *IET Image Process.*, 2012, **6**, (7), pp. 822–830

6 Starostenko, O., Chávez-Aragón, A., Burlak, G., Contreras, R.: 'A novel star field approach for shape indexing in CBIR system', *J. Eng. Lett.*, 2007, **1**, (2), pp. 10–21

7 Datta, R., Joshi, D., Li, J., Wang, J.: 'Image retrieval: ideas, influences, and trends of the new age', *ACM Comput. Surv.*, 2008, **40**, (2), pp. 1–60

8 Marakakis, A., Siolas, G., Galatsanos, N., Likas, A., Stafylopatis, A.: 'Relevance feedback approach for image retrieval combining support vector machines and adapted Gaussian mixture models', *IET Image Process.*, 2011, **5**, (6), pp. 531–574

9 Montagna, R., Finlayson, G.D.: 'Padua point interpolation and L^p-norm minimization in color-based image indexing and retrieval', *IET Image Process.*, 2012, **6**, pp. 139–147

10 Manjunath, B.S., Ohm, J.R., Vasudevan, V.V., Yamada, A.: 'Color and texture descriptors', *IEEE Trans. Circuits Syst. Video Technol.*, 2001, **11**, (6), pp. 703–715

11 Nixon, M., Aguado, A.: 'Feature extraction & image process', (Elsevier Ltd., 2002, 2nd edn.)

12 Young, C., Nam Chul, K., Ick Hoon, J.: 'Content-based image retrieval using multi-resolution color and texture features', *IEEE Trans. Multimed.*, 2008, **10**, (6), pp. 1073–1084

13 Vizireanu, D.N.: 'Morphological shape decomposition inter-frame interpolation method', *J. Electron. Imaging*, 2008, **17**, (1), pp. 1–5

14 Vizireanu, D.N.: 'Generalizations of binary morphological shape decomposition', *J. Electron. Imaging*, 2007, **16**, (1), pp. 1–6

15 Vizireanu, D.N., Halunga, S., Marghescu, G.: 'Morphological skeleton decomposition inter-frame interpolation method', *J. Electron. Imaging*, 2010, **19**, (2), pp. 1–3

16 Quellec, G., Lamard, M., Cazuguel, G., Cochener, B., Roux, C.: 'Fast wavelet-based image characterization for highly adaptive image retrieval', *IEEE Trans. Image Process.*, 2012, **21**, (4), pp. 1613–1623

17 Lakshmi, A., Rakshit, S.: 'New wavelet features for image indexing and retrieval'. IEEE Second Int. Advance Computing Conf., 2010, pp. 145–150

18 Hadamard matrix. Available at http://en.wikipedia.org/wiki/Hadamard_matrix

19 Funfzig, C., Ullrich, T., Fellner, D.W., Bachelder, E.N.: 'Terrain and model queries using scalar representations with wavelet compression', *IEEE Trans. Instrum. Meas.*, 2009, **58**, (9), pp. 3086–3093

20 Kekre, H.B., Thepade, S.D.: 'Using YUV color space to hoist the performance of block truncation coding for image retrieval'. Proc. IEEE-IACC'09, 2009, pp. 6–11

21 Corel Data set. Available at http://wang.ist.psu.edu/docs/related/ (last referred on 10 June 2009)

22 Geusebroek, J.M., Burghouts, G.J., Smeulders, A.W.M.: 'The Amsterdam library of object images', *Int. J. Comput. Vis.*, 2005, **61**, pp. 103–112

23 International organization for standardization, MPEG-7 overview 2004. Available at http://mpeg.chiariglione.org/standards/mpeg-7/mpeg-7.htm, accessed 15 November 2011

24 Veganzones, M.A., Graña, M.: 'A spectral/spatial CBIR system for hyper spectral images', *IEEE J. Sel. Top. Earth Obs. Remote Sens.*, 2012, **5**, pp. 488–500

25 Kekre, H.B., Mishra, D., Narula, S., Shah, V.: 'Color feature extraction for CBIR', *Int. J. Eng. Sci. Technol. (IJEST)*, 2011, **3**, (12), pp. 8375–8365

26 Troncy, R., Huet, B., Schenk, S.: 'Feature extraction for multimedia analysis: 'Multimedia semantics, desktop edition (XML): metadata, analysis and interaction' (John Wiley & Sons Inc., New York, 2011, 1st edn.), pp. 36–54

27 Jiang, Q., We, W., Zhang, H.: 'New researches about dominant color descriptor and graph edit distance'. Int. Conf. Intell. Human-Mach. Syst. and Cybernetics (IHMSC), 2011, vol. 1, pp. 50–52

doi: 10.1049/iet-ipr.2012.0203